
This is an electronic reprint of the original article.
This reprint may differ from the original in pagination and typographic detail.

Rösch, Johanna; Vetter, David Emanuel; Baldassarre, Antonello; Souza, Victor; Lioumis, Pantelis; Roine, Timo; Jooß, Andreas; Baur, David; Kozak, Gabor; Jovellar, D. Blair; Vaalto, Selja; Romani, Gian Luca; Ilmoniemi, Risto; Ziemann, Ulf

Individualized treatment of motor stroke : a perspective on open-loop, closed-loop and adaptive closed-loop brain state-dependent TMS

Published in:
Clinical Neurophysiology

DOI:
[10.1016/j.clinph.2023.10.004](https://doi.org/10.1016/j.clinph.2023.10.004)

E-pub ahead of print: 26/10/2023

Document Version
Peer-reviewed accepted author manuscript, also known as Final accepted manuscript or Post-print

Published under the following license:
CC BY-NC-ND

Please cite the original version:
Rösch, J., Vetter, D. E., Baldassarre, A., Souza, V., Lioumis, P., Roine, T., Jooß, A., Baur, D., Kozak, G., Jovellar, D. B., Vaalto, S., Romani, G. L., Ilmoniemi, R., & Ziemann, U. (2023). Individualized treatment of motor stroke : a perspective on open-loop, closed-loop and adaptive closed-loop brain state-dependent TMS. *Clinical Neurophysiology*. Advance online publication. <https://doi.org/10.1016/j.clinph.2023.10.004>

This material is protected by copyright and other intellectual property rights, and duplication or sale of all or part of any of the repository collections is not permitted, except that material may be duplicated by you for your research use or educational purposes in electronic or print form. You must obtain permission for any other use. Electronic or print copies may not be offered, whether for sale or otherwise to anyone who is not an authorised user.

1 **Individualized treatment of cortical stroke: a perspective on open-loop, closed-loop and**
2 **adaptive closed-loop brain state-dependent TMS**

3

4 Authors:

5 Johanna Rösch^{a,b,#}, David Emanuel Vetter^{a,b,#}, Antonello Baldassarre^c, Victor H. Souza^{d,e},
6 Pantelis Lioumis^{d,e}, Timo Roine^{d,e}, Andreas Jooß^{a,b}, David Baur^{a,b}, Gábor Kozák^{a,b}, D. Blair
7 Jovellar^{a,b}, Selja Vaalto^{d,f}, Gian Luca Romani^g, Risto J. Ilmoniemi^{d,e}, Ulf Ziemann^{a,b,*}

8

9 ^a Department of Neurology and Stroke, University of Tübingen, Tübingen, Germany

10 ^b Hertie-Institute for Clinical Brain Research, Tübingen, Germany

11 ^c Department of Neuroscience, Imaging and Clinical Sciences, University G. d'Annunzio of
12 Chieti-Pescara, Chieti, Italy

13 ^d Department of Neuroscience and Biomedical Engineering, Aalto University School of
14 Science, Espoo, Finland

15 ^e BioMag Laboratory, HUS Medical Imaging Center, University of Helsinki, Aalto University
16 and Helsinki University Hospital, Helsinki, Finland

17 ^f HUS Diagnostic Center, Clinical Neurophysiology, Clinical Neurosciences, Helsinki
18 University Hospital and University of Helsinki, Helsinki, Finland

19 ^g Institute for Advanced Biomedical Technologies, University of Chieti-Pescara, Chieti, Italy

20 # Contributed equally

21

22 * Corresponding author:

23 Ulf Ziemann

24 Eberhard Karls Universität Tübingen, Zentrum für Neurologie

25 Hertie-Institut für klinische Hirnforschung

26 Hoppe-Seyler-Straße 3, 72076 Tübingen

27 Tel. +49 7071 2982049

28 ulf.ziemann@uni-tuebingen.de

29

30 1. Closing the loop on stroke therapy

31 Stroke is a leading cause of disability in adults (Feigin et al., 2022; Katan and Luft, 2018),
32 affecting cognitive, language, or motor functions (Langhorne et al., 2011). Hence, validated
33 rehabilitation to improve post-stroke recovery of motor functions is in great demand. We here
34 argue that closed-loop transcranial magnetic stimulation (TMS) has potential in enhancing
35 rehabilitation, and will highlight the distinction between non-adaptive closed-loop TMS, and
36 adaptive closed-loop TMS. Briefly, non-adaptive closed-loop TMS aims at bringing a typical
37 patient's brain state to a desired target state and overcome expected perturbations. Adaptive
38 closed-loop TMS additionally offers the ability to adapt to individual patients and to
39 unexpected perturbations (Åström and Wittenmark, 2013). We also discuss how leveraging
40 state-of-the-art methods might support the implementation of these advanced TMS
41 rehabilitation approaches in the near future.

42 2. Investigating stroke recovery with neuroimaging methods

43 Motor function is tightly choreographed by the cerebral motor network, comprising the
44 primary motor cortex (M1), premotor cortex (PMC), supplementary motor area (SMA), the
45 cerebellum, and subcortical areas such as the thalamus (Rehme and Grefkes, 2013). Stroke
46 lesions in these areas do not only lead to a loss of function of the affected area but also
47 disrupt healthy motor network functioning (Baldassarre et al., 2016; Carrera and Tononi,
48 2014; Grefkes and Fink, 2014; Rehme and Grefkes, 2013; Siegel et al., 2022). There is no
49 one unique route of reorganization of the motor network after stroke to recover motor
50 function (Di Pino et al., 2014; Grefkes and Fink, 2014). Instead, we face a very
51 heterogeneous clinical population, where the path to recovery needs to be enhanced
52 individually (Di Pino et al., 2014; Ziemann et al., 2019). Identifying prognostic biomarkers
53 may be beneficial in selecting the individual therapeutic steps for motor recovery after stroke.

54 Potential biomarkers have been reported from different neuroimaging techniques:
55 magnetic resonance imaging (MRI) helps identify brain areas that are involved in motor
56 functions, and derived structural and functional connectivity analyses may help predict
57 individual patient recovery (Grefkes and Fink, 2014; Stinear, 2017). Magneto-
58 /electroencephalography (MEG/EEG), as neurophysiological methods, can furthermore
59 represent brain activity at a millisecond scale, enabling the coordination of interventions with
60 rapidly changing brain states.

61 Spontaneous EEG provides functional information characterized by activity in
62 different frequency bands: delta (0.5–4 Hz), theta (4–8 Hz), alpha (8–13 Hz), beta (13–30 Hz)
63 and gamma (>30 Hz) (Keser et al., 2022). Moreover, the so-called sensorimotor rhythm
64 refers to oscillations recorded over the sensorimotor cortex with peaks around 10 and 20 Hz
65 (Hari, 2006). In this paper, we relate to the alpha range (8–12 Hz) over the Rolandic fissure
66 when mentioning the mu-rhythm. Activity within frequency bands can be examined using
67 quantitative EEG measures derived from power spectrum analysis, and the relation of power
68 between different frequency bands (Finnigan and van Putten, 2013), or the functional
69 connectivity (FC) between different brain areas (Keser et al., 2022). The latter is commonly
70 calculated based on the coherence within given frequency bands between distant regions
71 (Keser et al., 2022). In view of stroke as a network disruption, FC seems to be a promising
72 tool to represent brain network changes that correspond to recovery. EEG can be combined
73 with non-invasive brain stimulation (NIBS) techniques, such as TMS (Hernandez-Pavon et
74 al., 2023; Kallioniemi and Daskalakis, 2022; Tremblay et al., 2019). Effective connectivity,
75 as investigated by combining EEG and TMS has potential to be a prognostic tool for stroke
76 recovery (Tecchio et al., 2023). TMS–EEG measures as predictive biomarkers have been
77 reviewed recently (Keser et al., 2022).

78 **3. Electrophysiological biomarkers in motor stroke**

79 In the following section, biomarkers in motor stroke are reviewed with a focus on FC
80 estimated from EEG-recorded data and frequency-based measures of EEG-power. Literature
81 on acute, sub-acute, and chronic stages of stroke as well as different types of stroke
82 (subcortical, cortical, ischemic, hemorrhagic) is considered. This overview covers only a
83 small part of the available publications; readers are referred to the literature that includes
84 more extensive reviews and more details (Finnigan and van Putten, 2013; Guggisberg et al.,
85 2019; Keser et al., 2022; Milani et al., 2022; Ulanov and Shtyrov, 2022).

86 3.1 Functional connectivity

87 EEG-derived FC reflects temporal correlations of the neurophysiological activity of remote
88 brain regions (Fingelkurts et al., 2005). There are several methods to calculate FC (Bastos
89 and Schoffelen, 2016) and it can further be examined with regard to inter- or intra-
90 hemispheric connectivity, which is of relevance in the approach of stroke as a network
91 disorder. Importantly for application in real-time settings, FC can be computed on the single-
92 trial level (Basti et al., 2022). Such FC metrics are not identical to the “traditional” trial-
93 average FC metrics. It is therefore important to note that the field of FC is heterogeneous;
94 results from one metric need not translate directly to other metrics. With this note of caution
95 in mind, we will briefly review how EEG-derived FC relates to stroke:

96 There is evidence that the reorganization of the imbalance in FC between and within
97 the hemispheres is related to motor recovery. Higher MEG-derived FC in the alpha band of
98 the ipsilesional primary somatosensory cortex and prefrontal cortex to the whole brain was
99 followed by better recovery, whereas reduced connectivity between contralesional
100 sensorimotor areas and the whole brain appears to be beneficial for motor recovery (Westlake
101 et al., 2012). In the sub-acute stage, lower inter-hemispheric connectivity between motor
102 cortices in the alpha band was detected in stroke patients with poor motor functions as

103 compared to healthy controls, together with an opposite pattern in the theta band (Kawano et
104 al., 2020). Calculation of the graph-theoretic weighted node degree, which reflects the
105 number of connections from different areas, has revealed that the global weighted node
106 degree between the ipsilesional motor cortex to other cortical areas correlates with motor
107 improvement within the first weeks after stroke, specific to the beta frequency band (Nicolo
108 et al., 2015). FC in the sensorimotor network, investigated in the beta band by normalized
109 inter-hemispheric strength, showed that lower beta is positively associated with corticospinal
110 tract integrity and upper extremity function (Pichiorri et al., 2018). Keser and colleagues
111 (2022) summarize that motor recovery is correlated with restoration of inter-hemispheric
112 activity with increased intra-hemispheric coherence in the ipsilesional motor network.

113 3.2 Power measures in different frequency bands

114 The brain symmetry index (BSI) in different frequency bands quantifies the similarity of
115 spectral power in EEG in the two hemispheres (van Putten, 2007). BSI, the amount of power
116 in different frequency bands as well as the ratios between bands, like the delta–alpha ratio
117 (DAR) or the ratio of delta+theta power to alpha+beta power (DTABR), are further methods
118 of so-called quantitative EEG to characterize brain activity (Kaiser, 2007).

119 Chronic stroke patients had higher BSI values in delta and theta bands in the
120 ipsilesional hemisphere compared to healthy controls, the increased asymmetry being
121 associated with poor motor outcome (Saes et al., 2019). In acute stroke patients, an increase
122 in relative delta power was observed, while healthy controls had higher relative alpha power,
123 which resulted in a higher DAR for the patients (Finnigan et al., 2016). Similarly, the
124 DTABR was higher in stroke patients due to higher relative beta power in the healthy
125 controls (Finnigan et al., 2016). In the sub-acute stage, DAR is positively correlated with the
126 National Institute of Health Stroke Scale (NIHSS) 30 days after the stroke event (Kwah and
127 Diong, 2014), which indicates that a greater amount of slower EEG components is associated

128 with more impairment (van Putten, 2007). Hence, reductions in delta power, DAR, DTABR
129 or BSI during the acute ischemic stroke stage are associated with relatively better functional
130 outcomes (Finnigan and van Putten, 2013).

131 Analyzing narrow bands in the frequency domain is often done without addressing the
132 aperiodic part of the signal, which is reflected in the decay of the EEG signal in the power
133 spectral density plots. Investigation of the steepness of the spectral exponent, which
134 represents broad-band EEG slowing, showed that slowing was more present in the affected
135 hemisphere of acute cortical stroke patients compared to healthy controls, and the difference
136 between the hemispheres became less two months after stroke ([Lanzone et al., 2022](#)). This
137 normalization further correlated with improvements on the NIHSS, which indicates that the
138 scale-free dimension of EEG can also be utilized as a marker of stroke recovery ([Lanzone et
139 al., 2022](#)).

140 4. Closed-loop TMS

141 TMS is a promising tool for motor stroke rehabilitation because of its ability to induce plastic
142 changes in the cortex (Ziemann et al., 2008). However, TMS effects on the motor system
143 suffer from inter- and intra-individual variability (Hamada et al., 2013). This is partially
144 explained by the cortical neuronal dynamics and endogenous network activity at the time of
145 the TMS pulse (Bergmann, 2018).

146 To address this variability, brain state-dependent stimulation protocols have been
147 developed, in which the TMS pulses are delivered in a time window when a selected brain
148 state occurs. In the motor system, the instantaneous phase and power of the mu-rhythm have
149 been identified as suitable indicators of opportune time windows (Bergmann et al., 2019;
150 Hussain et al., 2019, 2020; Karabanov et al., 2021; Sato et al., 2015; Schaworonkow et al.,
151 2018; Thies et al., 2018; Wischnewski et al., 2022; Zrenner et al., 2018, 2023). Stimulating

152 only during a specific target state can increase the efficacy of plasticity induction by TMS
153 (Baur et al., 2020; Zrenner et al., 2018).

154 Brain state-dependent stimulation can be performed in open- or closed-loop modes
155 (Antony et al., 2022): In open-loop brain state-dependent stimulation, pulses are delivered
156 when *a priori* defined target brain states are observed (Antony et al., 2022), e.g., at the trough
157 of the sensorimotor mu-rhythm (Schaworonkow et al., 2018). However, the immediate or
158 even long-term effect of the stimulation on the brain state is disregarded. In contrast, in
159 closed-loop brain state-dependent stimulation, this very effect of the stimulation is taken into
160 account by continuously adjusting the stimulation parameters such as the targeted brain state.
161 More precisely, the achieved outcome of the stimulus is compared against the desired
162 outcome, and the stimulation parameters are chosen based on this comparison. In non-
163 adaptive closed-loop control, this mapping from the deviation of the actual and the desired
164 outcome is fixed. In adaptive closed-loop control, it is continuously adjusted by an adaptation
165 mechanism (Åström, 1983). Adaptive closed-loop brain state-dependent stimulation may be a
166 critical addition in clinical settings, considering the very heterogeneous stroke population and
167 the highly variable recovery paths which are influenced by the type, location, and size of the
168 stroke lesion.

169 This paper aims to present a conceptual approach, illustrated by examples of experimental
170 set-ups, on how EEG biomarkers in adaptive closed-loop experiments can be utilized to
171 support motor recovery in stroke.

172 5. Strategy for TMS

173 Based on the aforementioned evidence on the association between EEG-based connectivity
174 and activity measures with motor outcome, it is possible to partially predict clinical recovery
175 from motor stroke using electrophysiological biomarkers. A straightforward strategy to
176 translate this into a therapy is to use TMS to enhance the expression of EEG biomarkers that

177 are predictive of good recovery, and suppress those that are predictive of unfavorable
178 outcomes. This way, the balance within the brain, disrupted by the lesion, may be restored.
179 However, it is likely that varying lesion locations (cortical vs. subcortical vs. subtentorial)
180 affect the EEG signal in different ways and to different extents, limiting the biomarkers that
181 can reliably be detected, and that stimulation methods and protocols need to be adjusted
182 depending on the individual patient and path of recovery (Di Pino et al., 2014).

183 5.1 Considerations on causality

184 We should note that a biomarker that correlates with recovery does not necessarily imply a
185 causal relationship with recovery. Nevertheless, experimentally testing the identified
186 (plausible) candidate biomarkers can reveal a causal relationship that may be used in therapy.
187 In a recent extensive review, Cassidy and colleagues investigated the complexity of
188 correlation and causation with regards to biomarkers based on FC in post-stroke recovery
189 (Cassidy et al., 2022). The authors utilize the Bradford Hill Criteria (Hill, 1965) to
190 demonstrate opportunities and challenges of connectivity biomarkers to predict post stroke
191 recovery (Cassidy et al., 2022).

192 In this context, TMS aiming to modulate an EEG biomarker of FC could provide the
193 strongest evidence that the biomarker causally supports post-stroke recovery.

194 5.2 Closing the control loop

195 Here, we follow previous literature that suggested using control approaches, especially
196 closed-loop control, to achieve better TMS efficacy (Antony et al., 2022; Zrenner et al.,
197 2016). As we aim to modify the brain with TMS in a way that an EEG biomarker changes,
198 we must ask: what control can we exert by TMS? This question has two aspects: first, we
199 need to characterize the stimulation parameter space; second, we need to characterize how
200 TMS affects the biomarker of interest. For concreteness, cohesiveness, and illustration, we
201 use EEG-derived FC as the biomarker of interest, without loss of generality.

202 5.2.1 The stimulation parameter space

203 The stimulation parameter space includes obvious parameters, such as the properties of the
204 induced electric field — its intensity, location of the highest field strength, and orientation.
205 With conventional TMS coils, this is defined by the coil geometry, position, and 3D
206 orientation (Deng et al., 2013; Opitz et al., 2011). With multi-coil transducers, the spatial
207 distribution of the induced electric field on the cortical surface can be adjusted electronically,
208 i.e., without physically moving the coils (Koponen et al., 2018; Nieminen et al., 2022; Nurmi
209 et al., 2021; Souza et al., 2022). Such multi-locus (mTMS) systems enable optimizing the
210 stimulation parameters with automated algorithms to achieve a target response on real-time
211 EEG and electromyographic recordings (Tervo et al., 2020, 2022). Additionally, the
212 waveform (mono- vs. biphasic) (Sommer et al., 2006) and duration (D’Ostilio et al., 2016) of
213 the TMS pulse contribute directly to the dynamics of the induced electric field and the
214 evoked brain response. Furthermore, the interval between consecutive TMS pulses
215 (interstimulus interval, ISI) constitutes another important stimulation parameter
216 (Hassanzahraee et al., 2019; Julkunen et al., 2012). TMS pulses can also be delivered in
217 trains, such as theta burst stimulation (TBS) (Chung et al., 2015). In this case, the duration
218 (e.g., 3 pulses) and internal frequency (e.g., 50 Hz) of the bursts, and the frequency at which
219 bursts are delivered (e.g., 5 Hz), as well as the number of bursts delivered continuously or in
220 series (e.g., continuous TBS vs. intermittent TBS; Chung et al., 2015; Huang et al., 2005;
221 Suppa et al., 2016) expand the stimulation parameter space substantially. Less obviously, the
222 state of the brain at the time of stimulation can be considered a stimulation parameter. By
223 giving the subject a suitable task, such as motor exercises or motor imagery in the case of
224 stroke patients, the effects of TMS may change because the motor network is already in an
225 active state (Hashimoto and Rothwell, 1999). In principle, the task during which TMS is

226 applied could thus be used to improve the efficacy of TMS, though this “task dynamics loop”
227 (Zrenner et al., 2016) will not be covered here.

228 TMS can also be triggered based on the spontaneous dynamics of the brain as
229 observed with EEG — in brain state-dependent stimulation. The brain state at which a pulse
230 is delivered thereby becomes another parameter of stimulation. For example, single pulses
231 have previously been delivered at specific phases of the sensorimotor mu-rhythm when there
232 was sufficient mu-band power (Schaworonkow et al., 2018). In such a case, the target
233 frequency band, the power threshold, and the target phase are also among the crucial
234 stimulation parameters. Clearly, the stimulation parameter space can be further expanded: for
235 example, brain states based on EEG phase synchronicity patterns in distributed networks
236 (Stefanou et al., 2018) or based on FC patterns may be identified and real-time inferences can
237 be developed.

238 5.2.2 Effects of TMS on functional connectivity

239 The goal we consider here is to modify FC with TMS in stroke patients suffering from a
240 cortical lesion. To achieve this, TMS needs to alter FC in specific connections and in a
241 defined direction. Open-loop brain state-independent TBS of M1 modifies the magnitude and
242 direction of resting-state FC depending on the TBS protocol. Whereas continuous TBS
243 decreased alpha-band FC across the whole cortex and increased beta-band FC between
244 bihemispheric anterior areas (Shafi et al., 2014), intermittent TBS increased alpha-band FC
245 (Zhang and Fong, 2021). Cortico–cortical paired associative stimulation can specifically
246 increase the high-beta FC along a target connection, by delivering paired pulses to the nodes
247 at either end of the connection (Hooyman et al., 2022). The orientation of the induced electric
248 field has also been demonstrated to affect FC measures (Pieramico et al., 2023). Thus, we
249 find it plausible that TMS is a suitable method to introduce specific, well-defined FC changes
250 in the motor network.

251 In the following, we will introduce both non-adaptive and adaptive closed-loop TMS
252 focused on FC with toy examples. These examples cannot directly be run as experiments yet,
253 but they will highlight which parts of the process are currently missing and need to be filled
254 in, in order to actually run such experiments.

255 5.3 Non-adaptive closed-loop brain stimulation

256 The notion of closed-loop control comes from control engineering and theory, and is for
257 example explained in detail in (Ogata, 2010). As has recently been highlighted, there is
258 substantial conflation of the terms closed-loop and brain state-dependent stimulation in the
259 field of TMS (Antony et al., 2022). The goal of closed-loop control is to control the system
260 state — driving the system or its response to a desired state by changing the stimulation
261 parameters based on the observed state. In the case of open-loop brain state-dependent
262 stimulation (e.g., triggering TMS on the trough of the mu rhythm), we affect the system
263 during a specific brain state with fixed or predefined parameters without updating them based
264 on measured effects. Such an open-loop stimulation may still alter the brain state, but this
265 effect is not taken into account in choosing the subsequent stimulation parameters.

266 In accordance with prior literature (Antony et al., 2022; Ogata, 2010; Thut et al.,
267 2017), we subscribe to the following definition: In closed-loop TMS, the stimulation
268 parameters are chosen based on the deviation of the observed brain-state from a reference,
269 i.e., a target brain state, to steer the brain state towards the reference. Therefore, closed-loop
270 TMS requires some predefined reference state and entails altering neuronal activity towards
271 that reference (Thut et al., 2017).

272 This reference could be derived *a priori* from the literature and medical knowledge,
273 but may, importantly, also be selected based on the individual medical needs of the patient. In
274 non-adaptive closed-loop control, the mapping of the deviation of the actual brain-state from
275 the reference to the stimulation parameters is static.

276 The non-adaptive closed-loop approach is detailed in Figure 1, with an illustrative
277 example (note that the example is speculative, and not strictly derived from prior literature):
278 let the reference state be a high FC between intra-hemispheric motor nodes (let those be SMA
279 and M1). This reference is then compared (not necessarily by subtraction) with the actual
280 brain state (e.g., low FC), yielding the deviation or error signal (e.g., “FC needs to be
281 increased”). This deviation is mapped onto stimulation parameters that are suitable to drive
282 the brain towards the reference state (e.g., intermittent TBS during low mu-power). This
283 mapping is called the “controller”, or control function (Figure 2, left panel). The stimulation
284 parameters are then translated into the actual stimuli by an “actuator”. The stimuli (e.g., 10
285 theta bursts) are delivered by the actuator to the brain—in control-engineering terms, they are
286 the control input to the system under control. The brain’s modified state in reaction to the
287 stimulation (e.g., slightly increased FC) is then observed in the EEG signal, and again
288 compared to the reference. Thereby, the loop is closed. If the control function is fixed, the
289 closed-loop control is called non-adaptive.

290 The brain state at which we deliver a pulse can be considered a stimulation parameter.
291 In that case, the real-time EEG processing system that infers the current brain state and
292 delivers a pulse when the selected brain state occurs, is (part of) the actuator and a tool of the
293 controller.

294 This example already highlights problems that need to be addressed when
295 implementing a closed-loop TMS protocol. Most prominently, the mapping from the
296 deviation of the actual brain state to the reference has to be chosen. In the simplest case, this
297 mapping might be manually defined led by prior knowledge. However, it might be more
298 feasible and flexible to infer it by machine learning: from simple linear regression to
299 generalized linear models to deep-learning based approaches (Gebodh et al., 2023). A wide

300 array of tools can be used to learn the mapping from an open-loop dataset. Naturally, this
301 requires a dataset that covers enough of the stimulation-parameter space.

302 Hitherto, the mapping from the error signal to the control input has been static — i.e.,
303 the parameters of the controller are fixed (Figure 1). While the stimulation parameters chosen
304 for too high FC may in general be different from those chosen when the FC is too low, the
305 stimulation parameters for a particular deviation will stay the same (Figure 2, left panel). That
306 is, the closed-loop control is non-adaptive. If this controller is then applied to a patient for
307 whom it does not fit, the protocol will fail. This motivates making the controller adaptive.

308 5.4 Adaptive closed-loop brain stimulation

309 In adaptive closed-loop brain stimulation, the mapping from deviation to stimulation
310 parameters is adapted on-line by an adjustment mechanism that takes the relation of control
311 input to the system and the system output into account (Åström, 1983). Hence, the mapping
312 of the deviation from the reference to stimulation parameters is no longer static, but
313 automatically adjusted.

314 The adaptive closed-loop brain stimulation approach is visualized in Figure 3, along
315 with a speculative example showing how it may be added to the above-described example of
316 non-adaptive closed-loop TMS. In this extended example, everything is the same from the
317 initial deviation to the first 10 theta bursts delivered. But now, let the original controller be
318 unfit to the patient: Instead of an increased FC (reduced deviation), we observe a further
319 decreased FC (increased deviation). In this case, if the controller remained static, it would
320 simply repeat the same inappropriate input, and would thus likely not achieve an increase in
321 FC. This is where the adjustment mechanism comes into play: the relation of the system input
322 (10 intermittent theta bursts at high intensity, during low mu-power) to the observed system
323 output (lower intra-hemispheric FC) is now used to modify the controller's parameters.

324 Figure 2 (right panel) illustrates an adjustment mechanism limited to the mapping
325 from the error signal to the targeted mu-band power, and ignores the other stimulation
326 parameters for the sake of brevity and illustration. The control function (dark red dashed line)
327 was fitted to prior data (calibration data; black dots) from representative patients. This might
328 for example be done by linear regression.

329 Since the aim is to increase FC (i.e., $\Delta FC > 0$ in Figure 2), the original mapping tells
330 us to target a low power state (see Figure 2, left panel, gray arrow). But as the system delivers
331 stimuli during low mu-power, we observe a decrease in FC — the opposite of what we
332 expected based on the calibration data. In the adaptive setting, we might, for example, replace
333 the first five data points of the calibration dataset with the five data points observed so far
334 from the deviant patient. Afterwards, the mapping is recomputed from the updated data by
335 linear regression — yielding a different mapping (see Figure 2, right panel). In this example,
336 the linear regression-based mapping would now recommend targeting an average or above-
337 average mu-power to increase FC, which is more appropriate for the simulated atypical
338 patient. That is, the controller’s parameters are being adapted to the system under control.
339 Note that in this example the parameters are frequently adjusted to the new patient.
340 Generally, the controller does not have to be adjusted after each “step”; it can be updated
341 more slowly (Åström and Wittenmark, 2013).

342 It should be evident already that there are many ways of implementing such an
343 adaptive controller. Naturally, other methods than linear regression may be used to select the
344 controller’s parameters. Furthermore, in the given example, the controller never “explores”, it
345 always “exploits”, and basically finds an improved mapping by luck and the convenience of
346 the given constructed example. This could, for instance, be addressed by an epsilon-greedy
347 policy or importance sampling (Sutton and Barto, 2018). These would allow the controller to

348 sample parts of the stimulation-parameter space that may not be of immediate interest for
349 controlling the system, but still may be important for system identification.

350 6. Conclusion and future directions

351 In this paper, we have highlighted the possibility to approach closed-loop brain stimulation in
352 an adaptive fashion when aiming for motor recovery in stroke patients. While the concept of
353 adaptive closed-loop stimulation itself is not new, we extend it with the integration of
354 electrophysiological biomarkers that can be bidirectionally modified by TMS. We do not
355 claim that only adaptive closed-loop stimulation is effective in improving motor recovery in
356 stroke patients. Instead, we seek to present and distinguish increasingly flexible approaches to
357 be employed, where they may become necessary. These approaches can be implemented in a
358 new fundamental way by novel algorithms for real-time data analysis, together with the
359 mTMS technology and methodology that we are currently developing (Souza et al., 2023;
360 Sinisalo et al., under review; Marzetti et al., under review; Humaidan et al., under review).

361 To establish therapeutic applications, dedicated research is needed. One apparent
362 question is, which biomarkers are of interest and sufficiently reliable, how these biomarkers
363 change over time after stroke and how they relate to recovery. Collecting and sharing suitable
364 large datasets will help address these questions collaboratively. This becomes crucial to draw
365 evidence-based conclusions, especially in the light of diverse connectivity measures.

366 Longitudinal studies that include patients and follow recovery for several months, from acute
367 to chronic stages, may help specify and customize biomarkers for different patient groups.

368 Studies aiming for causal relation instead of simple correlation can uncover brain
369 mechanisms that need to be targeted. Restoring the balance between and within the ipsi- and
370 contralesional hemispheres might play an important role (Grefkes and Fink, 2014). Another
371 important issue is the time after stroke when the stimulation is applied. Effectiveness and

372 therapy goals might be considerably different according to stroke stage, e.g., from prevention
373 of maladaptive changes in the early stage to supporting neuroplasticity at later stages.

374 Developments on TMS technology that enable rapid and multi-site stimulation is
375 crucial to modulate multiple nodes of a functional network. Recent advances in mTMS
376 systems (de Lara et al., 2021; Koponen et al., 2018; Nieminen et al., 2022; Souza et al., 2022)
377 enable one to adjust the stimulation parameters at a millisecond scale. This includes not only
378 intensity, timing, and wave shapes of the pulses but also the cortical target loci and induced
379 electric field orientation. These advanced systems could deliver the therapeutic stimulation at
380 the optimal brain state, to multiple brain regions of the unbalanced motor network after stroke
381 (Baldassarre et al., 2016; Grefkes and Fink, 2014; Rehme and Grefkes, 2013), thus allowing
382 the adjustment of far more parameters than the presently available instrumentation. This
383 approach would exploit the full potential of adaptive closed-loop algorithms, and may lead to
384 more effective treatments of network disorders than when stimulation is delivered at a single
385 cortical location.

386 If possible, neuroimaging methods such as functional or diffusion MRI can be
387 combined with MEG/ EEG methods to add to the overall diagnostic findings and to enable
388 more accurate mapping of the parameter space (Aydogan et al., 2023; Pieramico et al., 2023).
389 This may be especially necessary in cases where the latter methods fail to represent brain
390 activity accurately, such as focal, subcortical lesions (Finnigan and van Putten, 2013).

391 On the one hand, it is essential to define distinct characteristics of the selected
392 biomarkers that need to be targeted with a certain protocol. To this aim, computational
393 models might be employed to take into account the effects of focal lesion on the motor
394 network (Aerts et al., 2016). Moreover, the framework of closed-loop brain stimulation needs
395 to be translated into the clinical setting. Here the challenges relate to more practical issues. A
396 closed-loop stimulation approach should be built in such a way that it can reliably be applied

397 in the clinical environment with regard to the available equipment of medical institutions.

398 Also, human operators should retain control of the automated closed-loop applications.

399 Secondly, we want to highlight the importance of these medically trained human
400 operators: the choice of the reference state (goal of therapy) should be informed by the needs
401 of the patient, the structural and functional lesions in the patient’s brain and associated motor
402 impairments. This may eventually be supported or even completely done by autonomous
403 systems, but likely will for now and a long time remain at least partially the domain of
404 humans. This means that it is not necessary for clinical applications to have a fully
405 autonomous system based on machine learning — partial automation can already be very
406 useful for clinical practice. Even when high-level decisions remain the field of human
407 operators, automated algorithms that select and adjust the stimulation parameters in real time
408 serve a crucial role in minimizing user-dependent errors (Nieminen et al., 2022; Tervo et al.,
409 2022), and are a first step towards higher levels of autonomy as has been achieved in surgical
410 robotics (Attanasio et al., 2021).

411 Adaptive closed-loop brain stimulation holds the potential to address the
412 heterogeneity of the clinical population and to enhance motor recovery in stroke patients.
413 Finally, motor stroke is just one example of a brain network disorder, but many other
414 frequent neurological and psychiatric diseases, such as Alzheimer’s disease, Parkinson’s
415 disease, multiple sclerosis, depression, obsessive compulsive disorder, anxiety disorder,
416 addiction or pain can be conceptualized as network disorders that can also be targeted by
417 adaptive closed-loop brain stimulation in a highly individualized manner.

418

419 **Acknowledgement**

420 This concept paper is part of the ConnectToBrain project that has received funding from the
421 European Research Council (ERC) under the European Union's Horizon 2020 research and
422 innovation programme (Grant agreement No. 810377). This concept paper should be
423 considered in conjunction with the other three concept papers illustrating the ongoing
424 activities that are carried out and that, altogether, constitute the overall investigation of the
425 ConnectToBrain project.

426 V.H.S. has received funding from the Academy of Finland (decision No. 349985).

427

428 J.R. and D.E.V. contributed equally to the manuscript. D.E.V. created the figures,
429 incorporating feedback from V.H.S.. All authors discussed the presented concept, made
430 adjustments, revised the manuscript and approved its final version.

431

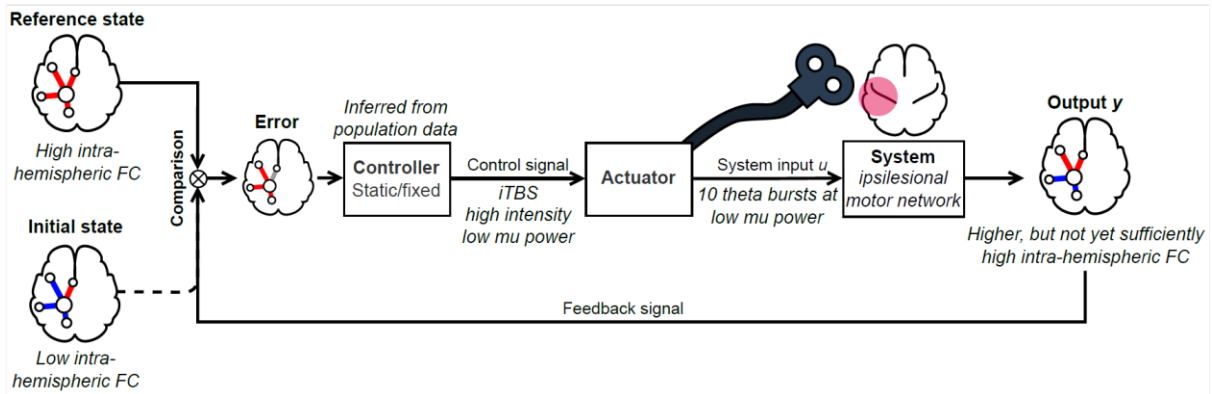
432 **Declaration of competing interests**

433 Risto J. Ilmoniemi is a patent holder for mTMS-related technology. All other authors declare
434 no competing interests.

435

436 **Figures**

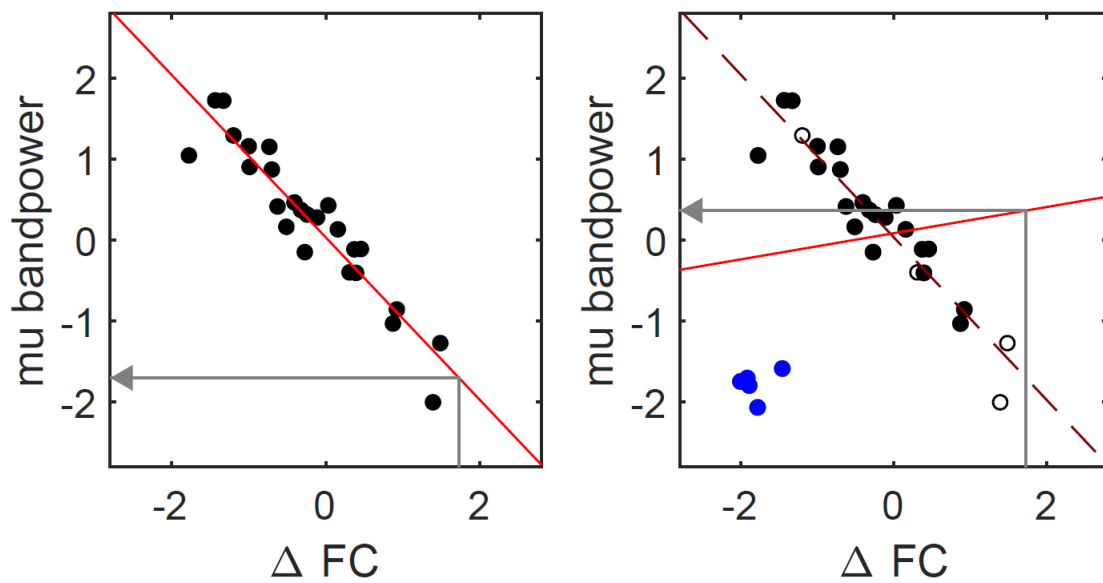
437



438

439 [CAPTION] FIGURE 1 Non-adaptive closed-loop control. General depiction of a non-
 440 adaptive closed-loop controller, with values from a speculative example for illustration: The
 441 reference (high intra-hemispheric functional connectivity (FC)) is compared to the initial
 442 system output (low intra-hemispheric FC), yielding the error signal (“FC needs to be
 443 increased”). The error signal is mapped onto the stimulation parameters by the controller
 444 (intermittent theta burst stimulation (iTBS), high intensity, low mu-power). The stimulation
 445 parameters are translated into the actual system input (10 theta bursts at low mu-power) by
 446 the actuator. The system (ipsilesional motor network of a motor stroke patient) then gives
 447 some output (increased, but low intra-hemispheric FC) in response to this input. The output is
 448 fed back to the comparison with the reference (closed-loop). Note that the controller’s
 449 parameters are fixed/static (non-adaptive). [END CAPTION]

450



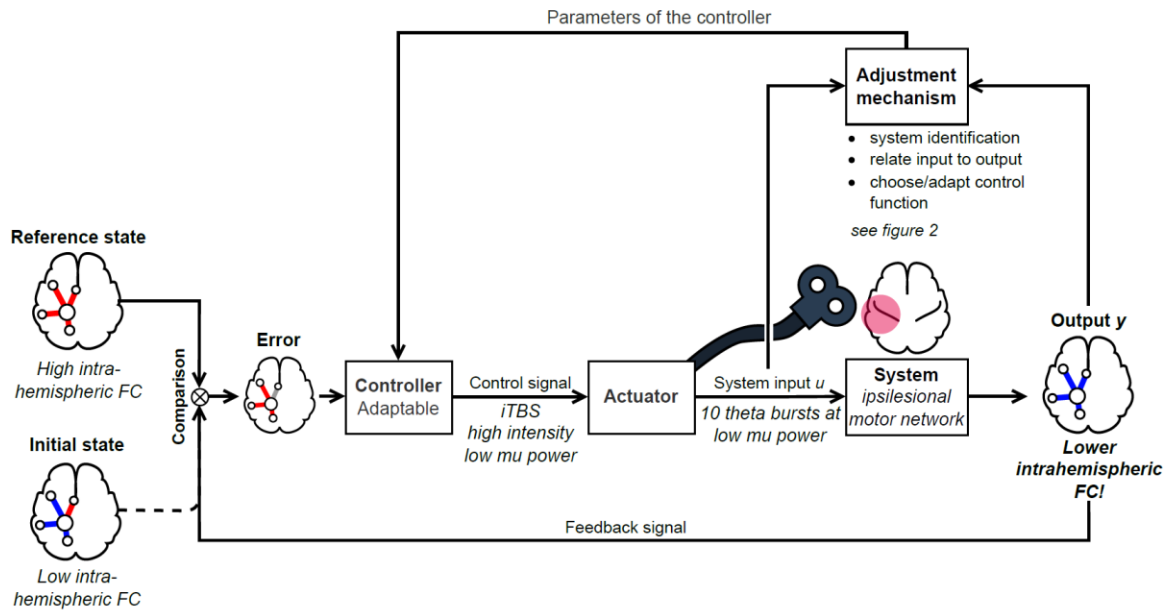
451

452 [CAPTION] FIGURE 2 Illustrative example of an adjustment mechanism (explanation see
 453 4.4).

454 Left: the parameters of the controller (i.e., the mapping from error to control signal; red line)
 455 are inferred from a calibration dataset (black dots). The gray arrow in the left plot indicates
 456 how the desired change in functional connectivity (FC) ($\Delta FC > 0$) is mapped to the target low
 457 mu-power (see examples in 4.3 and 4.4, and Figures 1 and 3). Right: new observations (blue
 458 dots) sampled at this target band-power replace some of the calibration data (black circles),
 459 and the controller's parameters are re-inferred (red line). The updated controller thus will
 460 pick a different target mu-power to achieve the same change in FC (gray arrow).

461 All data here presented are fictional. [END CAPTION]

462



463

464 [CAPTION] FIGURE 3 Adaptive closed-loop control. General depiction of an adaptive
 465 closed-loop controller: the reference is compared to the system output, yielding the error
 466 signal. The error signal is mapped onto the stimulation parameters by the controller. The
 467 stimulation parameters are translated into the actual system input by the actuator (intermittent
 468 theta burst stimulation (iTBS)). The system then gives some output in response to this
 469 input. The output is fed back to the comparison with the reference (closed-loop). An
 470 adjustment mechanism further relates system input/ stimulation parameters and output, and
 471 on this basis can adjust the parameters of the controller, making it adaptive. The concrete,
 472 illustrative values are nearly the same as in Figure 1, however, in this case, the result of the
 473 stimulation is lower intra-hemispheric functional connectivity (FC), because the controller is
 474 here applied to an unfit patient. The adjustment mechanism is illustrated in Figure 2. [END
 475 CAPTION]

476

477 **References**

478 Aerts, H., Fias, W., Caeyenberghs, K., Marinazzo, D. (2016). Brain networks under attack:
479 robustness properties and the impact of lesions. *Brain*, 139(12), 3063–3083.
480 <https://doi.org/10.1093/brain/aww194>

481 Antony, J. W., Ngo, H.-V. V., Bergmann, T. O., Rasch, B. (2022). Real-time, closed-loop, or
482 open-loop stimulation? Navigating a terminological jungle. *J. Sleep Res.*, 31(6), e13755.
483 <https://doi.org/10.1111/jsr.13755>

484 Åström, K. J. (1983). Theory and applications of adaptive control—a survey. *automatica*,
485 19(5), 471–486. [https://doi.org/10.1016/0005-1098\(83\)90002-X](https://doi.org/10.1016/0005-1098(83)90002-X)

486 Åström, K. J., Wittenmark B. (2013). *Adaptive control* (2nd ed.). Dover Publications, INC.

487 Attanasio, A., Scaglioni, B., De Momi, E., Fiorini, P., Valdastrì, P. (2021). Autonomy in
488 surgical robotics. *Annu. Rev. Control Robot. Auton. Syst.*, 4, 651–679.
489 <https://doi.org/10.1146/annurev-control-062420-090543>

490 Aydogan, D. B., Souza, V. H., Matsuda, R. H., Lioumis, P., Ilmoniemi, R. J. (2023). Real-
491 time tractography-assisted neuronavigation for TMS. *BioRxiv*, 2023-03.

492 Baldassarre, A., Ramsey, L., Rengachary, J., Zinn, K., Siegel, J. S., Metcalf, N. V., Strube,
493 M. J., Snyder, A. Z., Corbetta, M., Shulman, G. L. (2016). Dissociated functional
494 connectivity profiles for motor and attention deficits in acute right-hemisphere stroke. *Brain*,
495 139(7), 2024–2038. <https://doi.org/10.1093/brain/aww107>

496 Basti, A., Chella, F., Guidotti, R., Ermolova, M., D’Andrea, A., Stenroos, M., Romani, G.L.,
497 Pizzella, V., Marzetti, L. (2022). Looking through the windows: a study about the
498 dependency of phase-coupling estimates on the data length. *J. Neural Eng.*, 19(1), 016039.

499 Bastos, A. M., Schoffelen, J. M. (2016). A tutorial review of functional connectivity analysis
500 methods and their interpretational pitfalls. *Front. Syst. Neurosci.*, 9(175).
501 <https://doi.org/10.3389/fnsys.2015.00175>

502 Baur, D., Galevska, D., Hussain, S., Cohen, L. G., Ziemann, U., Zrenner, C. (2020).
503 Induction of LTD-like corticospinal plasticity by low-frequency rTMS depends on pre-
504 stimulus phase of sensorimotor μ -rhythm. *Brain Stimul.*, 13(6), 1580–1587.
505 <https://doi.org/10.1016/j.brs.2020.09.005>

506 Bergmann, T. O. (2018). Brain state-dependent brain stimulation. *Front. Psychol.*, 9, 2108.
507 <https://doi.org/10.3389/fpsyg.2018.02108>

508 Bergmann, T. O., Lieb, A., Zrenner, C., Ziemann, U. (2019). Pulsed facilitation of
509 corticospinal excitability by the sensorimotor μ -alpha rhythm. *J. Neurosci.*, 39(50), 10034–
510 10043. <https://doi.org/10.1523/JNEUROSCI.1730-19.2019>

511 Carrera, E., Tononi, G. (2014). Diaschisis: past, present, future. *Brain*, 137(9), 2408–2422.
512 <https://doi.org/10.1093/brain/awu101>

513 Cassidy, J. M., Mark, J. I., Cramer, S. C. (2022). Functional connectivity drives stroke
514 recovery: shifting the paradigm from correlation to causation. *Brain*, 145(4), 1211–1228.
515 <https://doi.org/10.1093/brain/awab469>

516 Chung, S. W., Hoy, K. E., Fitzgerald, P. B. (2015). Theta-burst stimulation: a new form of
517 TMS treatment for depression?. *Depress. Anxiety*, 32(3), 182–192.
518 <https://doi.org/10.1002/da.22335>

519 D’Ostilio, K., Goetz, S. M., Hannah, R., Ciocca, M., Chieffo, R., Chen, J. C. A., Peterchev,
520 A. V., Rothwell, J. C. (2016). Effect of coil orientation on strength-duration time constant

521 and I-wave activation with controllable pulse parameter transcranial magnetic stimulation.
522 *Clin. Neurophysiol.*, 127(1), 675–683. <https://doi.org/10.1016/j.clinph.2015.05.017>

523 de Lara, L. I. N., Daneshzand, M., Mascarenas, A., Paulson, D., Pratt, K., Okada, Y., Raij, T.,
524 Makarov, S. N., Nummenmaa, A. (2021). A 3-axis coil design for multichannel TMS arrays.
525 *NeuroImage*, 224, 117355. <https://doi.org/10.1016/j.neuroimage.2020.117355>

526 Deng, Z. D., Lisanby, S. H., Peterchev, A. V. (2013). Electric field depth-focality tradeoff in
527 transcranial magnetic stimulation: simulation comparison of 50 coil designs. *Brain Stimul.*,
528 6(1), 1–13. <https://doi.org/10.1016/j.brs.2012.02.005>

529 Di Pino, G., Pellegrino, G., Assenza, G., Capone, F., Ferreri, F., Formica, D., Ranieri, F.,
530 Tombini, M., Ziemann, U., Rothwell, J. C., Di Lazzaro, V. (2014). Modulation of brain
531 plasticity in stroke: a novel model for neurorehabilitation. *Nat. Rev. Neurol.*, 10(10), 597–
532 608. <https://doi.org/10.1038/nrneurol.2014.162>

533 Feigin, V. L., Brainin, M., Norrving, B., Martins, S., Sacco, R. L., Hacke, W., Fisher, M.,
534 Pandian, J., Lindsay, P. (2022). World stroke organization (WSO): global stroke fact sheet
535 2022. *Int. J. Stroke*, 17(1), 18–29. <https://doi.org/10.1177/17474930211065917>

536 Fingelkurts, A. A., Fingelkurts, A. A., Kähkönen, S. (2005). Functional connectivity in the
537 brain—is it an elusive concept?. *Neurosci. Biobehav. Rev.*, 28(8), 827–836.

538 Finnigan, S., van Putten, M. J. A. M. (2013). EEG in ischaemic stroke: quantitative EEG can
539 uniquely inform (sub-) acute prognoses and clinical management. *Clin. Neurophysiol.*,
540 124(1), 10–19. <https://doi.org/10.1016/j.clinph.2012.07.003>

541 Finnigan, S., Wong, A., Read, S. (2016). Defining abnormal slow EEG activity in acute
542 ischaemic stroke: delta/alpha ratio as an optimal QEEG index. *Clin. Neurophysiol.*, *127*(2),
543 1452–1459. <https://doi.org/10.1016/j.clinph.2015.07.014>

544 Gebodh, N., Miskovic, V., Laszlo, S., Datta, A., Bikson, M. (2023). A scalable framework
545 for closed-loop neuromodulation with deep learning. *BioRxiv*. 2023-01.
546 <https://doi.org/10.1101/2023.01.18.524615>

547 Grefkes, C., Fink, G. R. (2014). Connectivity-based approaches in stroke and recovery of
548 function. *Lancet Neurol.*, *13*(2), 206-216. [https://doi.org/10.1016/S1474-4422\(13\)70264-3](https://doi.org/10.1016/S1474-4422(13)70264-3)

549 Guggisberg, A. G., Koch, P. J., Hummel, F. C., Buetefisch, C. M. (2019). Brain networks and
550 their relevance for stroke rehabilitation. *Clin. Neurophysiol.*, *130*(7), 1098–1124.
551 <https://doi.org/10.1016/j.clinph.2019.04.004>

552 Hamada, M., Murase, N., Hasan, A., Balaratnam, M., Rothwell, J. C. (2013). The role of
553 interneuron networks in driving human motor cortical plasticity. *Cereb. Cortex*, *23*(7), 1593–
554 1605. <https://doi.org/10.1093/cercor/bhs147>

555 Hari, R. (2006). Action-perception connection and the cortical mu rhythm. *Prog. Brain Res.*,
556 *159*, 253–260. [https://doi.org/10.1016/S0079-6123\(06\)59017-X](https://doi.org/10.1016/S0079-6123(06)59017-X)

557 Hashimoto, R., Rothwell, J. C. (1999). Dynamic changes in corticospinal excitability during
558 motor imagery. *Exp. Brain Res.*, *125*, 75–81.

559 Hassanzahraee, M., Zoghi, M., Jaberzadeh, S. (2019). Longer transcranial magnetic
560 stimulation intertrial interval increases size, reduces variability, and improves the reliability
561 of motor evoked potentials. *Brain Connect.*, *9*(10), 770–776.
562 <https://doi.org/10.1089/brain.2019.0714>

563 Hernandez-Pavon, J. C., Veniero, D., Bergmann, T. O., Belardinelli, P., Bortoletto, M.,
564 Casarotto, S., Casula, E. P., Farzan, F., Fecchio, M., Julkunen, P., Kallioniemi, E., Lioumis,
565 P., Metsomaa, J., Miniussi, C., Mutanen, T. P., Rocchi, L., Rogasch, N. C., Shafi, M. M.,
566 Siebner, H. R., Thut, G., Zrenner, C., Ziemann, U., Ilmoniemi, R. J. (2023). TMS combined
567 with EEG: recommendations and open issues for data collection and analysis. *Brain Stimul.*,
568 *16*(2), 567-593. <https://doi.org/10.1016/j.brs.2023.02.009>

569 Hill, A. (1965). The environment and disease: association or causation?. *Proc. R. Soc. Med.*,
570 *58*(5), 295–300.

571 Hooyman, A., Garbin, A., Fisher, B. E., Kutch, J. J., Winstein, C. J. (2022). Paired
572 associative stimulation applied to the cortex can increase resting-state functional
573 connectivity: a proof of principle study. *Neurosci. Lett.*, *784*, 136753.
574 <https://doi.org/https://doi.org/10.1016/j.neulet.2022.136753>

575 Huang, Y. Z., Edwards, M. J., Rounis, E., Bhatia, K. P., Rothwell, J. C. (2005). Theta burst
576 stimulation of the human motor cortex. *Neuron*, *45*(2), 201–206.
577 <https://doi.org/10.1016/j.neuron.2004.12.033>

578 Hussain, S. J., Claudino, L., Bönstrup, M., Norato, G., Cruciani, G., Thompson, R., Zrenner,
579 C., Ziemann, U., Buch, E., Cohen, L. G. (2019). Sensorimotor oscillatory phase-power
580 interaction gates resting human corticospinal output. *Cereb. Cortex*, *29*(9), 3766–3777.
581 <https://doi.org/10.1093/cercor/bhy255>

582 Hussain, S. J., Hayward, W., Fourcand, F., Zrenner, C., Ziemann, U., Buch, E. R., Hayward,
583 M. K., Cohen, L. G. (2020). Phase-dependent transcranial magnetic stimulation of the
584 lesioned hemisphere is accurate after stroke. *Brain Stimul.*, *13*(5), 1354–1357.
585 <https://doi.org/10.1016/j.brs.2020.07.005>

586

587 Julkunen, P., Säisänen, L., Hukkanen, T., Danner, N., Könönen, M. (2012). Does second-
588 scale intertrial interval affect motor evoked potentials induced by single-pulse transcranial
589 magnetic stimulation?. *Brain Stimul.*, 5(4), 526–532.

590 <https://doi.org/10.1016/j.brs.2011.07.006>

591 Kaiser, D. A. (2007). What is quantitative EEG?. *J. Neurother.*, 10(4), 37–52.

592 https://doi.org/10.1300/J184v10n04_05

593 Kallioniemi, E., Daskalakis, Z. J. (2022). Identifying novel biomarkers with TMS-EEG –
594 methodological possibilities and challenges. *J. Neurosci. Methods*, 377, 109631.

595 <https://doi.org/https://doi.org/10.1016/j.jneumeth.2022.109631>

596 Karabanov, A. N., Madsen, K. H., Krohne, L. G., Siebner, H. R. (2021). Does pericentral mu-
597 rhythm “power” corticomotor excitability? – a matter of EEG perspective. *Brain Stimul.*,

598 14(3), 713–722. <https://doi.org/10.1016/j.brs.2021.03.017>

599 Katan, M., Luft, A. (2018). Global burden of stroke. *Semin. Neurol.*, 38(2), 208–211.

600 <https://doi.org/10.1055/s-0038-1649503>

601 Kawano, T., Hattori, N., Uno, Y., Hatakenaka, M., Yagura, H., Fujimoto, H., Yoshioka, T.,

602 Nagasako, M., Otomune, H., Kitajo, K., Miyai, I. (2020). Electroencephalographic phase

603 synchrony index as a biomarker of poststroke motor impairment and recovery. *Neurorehab.*

604 *Neural Re.*, 34(8), 711–722. <https://doi.org/10.1177/1545968320935820>

605 Keser, Z., Buchl, S. C., Seven, N. A., Markota, M., Clark, H. M., Jones, D. T., Lanzino, G.,

606 Brown, R. D., Worrell, G. A., Lundstrom, B. N. (2022). Electroencephalogram (EEG) with or

607 without transcranial magnetic stimulation (TMS) as biomarkers for post-stroke recovery: a
608 narrative review. *Front. Neurol.*, *13*, 827866. <https://doi.org/10.3389/fneur.2022.827866>

609 Koponen, L. M., Nieminen, J. O., Ilmoniemi, R. J. (2018). Multi-locus transcranial magnetic
610 stimulation—theory and implementation. *Brain Stimul.*, *11*(4), 849–855.
611 <https://doi.org/10.1016/j.brs.2018.03.014>

612 Kwah, L. K., Diong, J. (2014). National institutes of health stroke scale (NIHSS). *J.*
613 *Physiother.*, *60*(1), 61. <https://doi.org/10.1016/j.jphys.2013.12.012>

614 Langhorne, P., Bernhardt, J., Kwakkel, G. (2011). Stroke rehabilitation. *Lancet*, *377*(9778),
615 1693–1702. [https://doi.org/10.1016/S0140-6736\(11\)60325-5](https://doi.org/10.1016/S0140-6736(11)60325-5)

616 Lanzone, J., Colombo, M. A., Sarasso, S., Zappasodi, F., Rosanova, M., Massimini, M., Di
617 Lazzaro, V., Assenza, G. (2022). EEG spectral exponent as a synthetic index for the
618 longitudinal assessment of stroke recovery. *Clin. Neurophysiol.*, *137*, 92-101.
619 <https://doi.org/10.1016/j.clinph.2022.02.022>

620 Milani, G., Antonioni, A., Baroni, A., Malerba, P., Straudi, S. (2022). Relation between EEG
621 measures and upper limb motor recovery in stroke patients: a scoping review. *Brain Topogr.*,
622 *35*(5–6), 651–666. <https://doi.org/10.1007/s10548-022-00915-y>

623 Nicolo, P., Rizk, S., Magnin, C., Pietro, M. Di, Schnider, A., Guggisberg, A. G. (2015).
624 Coherent neural oscillations predict future motor and language improvement after stroke.
625 *Brain*, *138*(10), 3048–3060. <https://doi.org/10.1093/brain/awv200>

626 Nieminen, J. O., Sinisalo, H., Souza, V. H., Malmi, M., Yuryev, M., Tervo, A. E., Stenroos,
627 M., Milardovich, D., Korhonen, J. T., Koponen, L. M., Ilmoniemi, R. J. (2022). Multi-locus

628 transcranial magnetic stimulation system for electronically targeted brain stimulation. *Brain*
629 *Stimul.*, 15(1), 116–124. <https://doi.org/10.1016/j.brs.2021.11.014>

630 Nurmi, S., Karttunen, J., Souza, V. H., Ilmoniemi, R. J., Nieminen, J. O. (2021). Trade-off
631 between stimulation focality and the number of coils in multi-locus transcranial magnetic
632 stimulation. *J. Neural Eng.*, 18(6), 066003. <https://doi.org/10.1088/1741-2552/ac3207>

633 Ogata, K. (2010). Modern control engineering. In *Modern Control Engineering* (5th ed.).
634 Prentice Hall.

635 Opitz, A., Windhoff, M., Heidemann, R. M., Turner, R., Thielscher, A. (2011). How the brain
636 tissue shapes the electric field induced by transcranial magnetic stimulation. *NeuroImage*,
637 58(3), 849–859. <https://doi.org/10.1016/j.neuroimage.2011.06.069>

638 Pichiorri, F., Petti, M., Caschera, S., Astolfi, L., Cincotti, F., Mattia, D. (2018). An EEG
639 index of sensorimotor interhemispheric coupling after unilateral stroke: clinical and
640 neurophysiological study. *Eur. J. Neurosci.*, 47(2), 158–163.
641 <https://doi.org/10.1111/ejn.13797>

642 Pieramico, G., Guidotti, R., Nieminen, A. E., Andrea, A. D., Basti, A., Souza, V. H.,
643 Nieminen, J. O., Lioumis, P., Ilmoniemi, R. J., Romani, G. L., Pizzella, V., Marzetti, L.
644 (2023). TMS-induced modulation of EEG functional connectivity is affected by the E-field
645 orientation. *Brain Sci.*, 13(3), 418.

646 Rehme, A. K., Grefkes, C. (2013). Cerebral network disorders after stroke: evidence from
647 imaging-based connectivity analyses of active and resting brain states in humans. *J. Physiol.*,
648 591(1), 17–31. <https://doi.org/10.1113/jphysiol.2012.243469>

649 Saes, M., Meskers, C. G. M., Daffertshofer, A., de Munck, J. C., Kwakkel, G., van Wegen, E.
650 E. H. (2019). How does upper extremity Fugl-Meyer motor score relate to resting-state EEG
651 in chronic stroke? A power spectral density analysis. *Clin. Neurophysiol.*, *130*(5), 856–862.
652 <https://doi.org/10.1016/j.clinph.2019.01.007>

653 Sato, S., Bergmann, T. O., Borich, M. R. (2015). Opportunities for concurrent transcranial
654 magnetic stimulation and electroencephalography to characterize cortical activity in stroke.
655 *Front. Hum. Neurosci.*, *9*, 250. <https://doi.org/10.3389/fnhum.2015.00250>

656 Schaworonkow, N., Caldana Gordon, P., Belardinelli, P., Ziemann, U., Bergmann, T. O.,
657 Zrenner, C. (2018). μ -rhythm extracted with personalized EEG filters correlates with
658 corticospinal excitability in real-time phase-triggered EEG-TMS. *Front. Neurosci.*, *12*, 954.
659 <https://doi.org/10.3389/fnins.2018.00954>

660 Shafi, M. M., Brandon Westover, M., Oberman, L., Cash, S. S., Pascual-Leone, A. (2014).
661 Modulation of EEG functional connectivity networks in subjects undergoing repetitive
662 transcranial magnetic stimulation. *Brain Topogr.*, *27*, 172–191.
663 <https://doi.org/10.1007/s10548-013-0277-y>

664 Siegel, J. S., Shulman, G. L., Corbetta, M. (2022). Mapping correlated neurological deficits
665 after stroke to distributed brain networks. *Brain Struct. Funct.*, *227*(9), 3173–3187.

666 Sommer, M., Alfaro, A., Rummel, M., Speck, S., Lang, N., Tings, T., Paulus, W. (2006).
667 Half sine, monophasic and biphasic transcranial magnetic stimulation of the human motor
668 cortex. *Clin. Neurophysiol.*, *117*(4), 838–844. <https://doi.org/10.1016/j.clinph.2005.10.029>

669 Souza, V. H., Nieminen, J. O., Tugin, S., Koponen, L. M., Baffa, O., Ilmoniemi, R. J. (2022).
670 TMS with fast and accurate electronic control: measuring the orientation sensitivity of

671 corticomotor pathways. *Brain Stimul.*, 15(2), 306–315.
672 <https://doi.org/10.1016/j.brs.2022.01.009>

673 Souza, V. H., Sinisalo, H., Korhonen, J. K., Paasonen, J., Nyrhinen, M., Nieminen, J. O.,
674 Koponen, M., Kettunen, M., Gröhn, O., Ilmoniemi, R. J. (2023). A multi-channel TMS
675 system enabling accurate stimulus orientation control during concurrent ultra-high-field MRI
676 for preclinical applications. *BioRxiv*, 2023-08. <https://doi.org/10.1101/2023.08.10.552401>

677 Stefanou, M. I., Desideri, D., Belardinelli, P., Zrenner, C., Ziemann, U. (2018). Phase
678 synchronicity of μ -rhythm determines efficacy of interhemispheric communication between
679 human motor cortices. *J. Neurosci.*, 38(49), 10525–10534.
680 <https://doi.org/10.1523/JNEUROSCI.1470-18.2018>

681 Stinear, C. M. (2017). Prediction of motor recovery after stroke: advances in biomarkers.
682 *Lancet Neurol.*, 16(10), 826–836. [https://doi.org/10.1016/S1474-4422\(17\)30283-1](https://doi.org/10.1016/S1474-4422(17)30283-1)

683 Suppa, A., Huang, Y. Z., Funke, K., Ridding, M. C., Cheeran, B., Di Lazzaro, V., Ziemann,
684 U., Rothwell, J. C. (2016). Ten years of theta burst stimulation in humans: established
685 knowledge, unknowns and prospects. *Brain Stimul.*, 9(3), 323–335.
686 <https://doi.org/10.1016/j.brs.2016.01.006>

687 Sutton, R. S., Barto, A. G. (2018). Reinforcement learning: an introduction. *MIT press*.

688 Tecchio, F., Giambattistelli, F., Porcaro, C., Cottone, C., Mutanen, T. P., Pizzella, V.,
689 Marzetti, L., Ilmoniemi, R. J., Vernieri, F., Rossini, P. M. (2023). Effective intracerebral
690 connectivity in acute stroke: a TMS–EEG study. *Brain Sci.*, 13(2), 233.
691 <https://doi.org/10.3390/brainsci13020233>

692 Tervo, A. E., Metsomaa, J., Nieminen, J. O., Sarvas, J., Ilmoniemi, R. J. (2020). Automated
693 search of stimulation targets with closed-loop transcranial magnetic stimulation. *NeuroImage*,
694 220, 117082. <https://doi.org/10.1016/j.neuroimage.2020.117082>

695 Tervo, A. E., Nieminen, J. O., Lioumis, P., Metsomaa, J., Souza, V. H., Sinisalo, H.,
696 Stenroos, M., Sarvas, J., Ilmoniemi, R. J. (2022). Closed-loop optimization of transcranial
697 magnetic stimulation with electroencephalography feedback. *Brain Stimul.*, 15(2), 523–531.
698 <https://doi.org/10.1016/j.brs.2022.01.016>

699 Thies, M., Zrenner, C., Ziemann, U., Bergmann, T. O. (2018). Sensorimotor mu-alpha power
700 is positively related to corticospinal excitability. *Brain Stimul.*, 11(5), 1119–1122.
701 <https://doi.org/10.1016/j.brs.2018.06.006>

702 Thut, G., Bergmann, T. O., Fröhlich, F., Soekadar, S. R., Brittain, J. S., Valero-Cabré, A.,
703 Sack, A. T., Miniussi, C., Antal, A., Siebner, H. R., Ziemann, U., Herrmann, C. S. (2017).
704 Guiding transcranial brain stimulation by EEG/MEG to interact with ongoing brain activity
705 and associated functions: a position paper. *Clin. Neurophysiol.*, 128(5), 843–857.
706 <https://doi.org/10.1016/j.clinph.2017.01.003>

707 Tremblay, S., Rogasch, N. C., Premoli, I., Blumberger, D. M., Casarotto, S., Chen, R., Di
708 Lazzaro, V., Farzan, F., Ferrarelli, F., Fitzgerald, P. B., Hui, J., Ilmoniemi, R. J., Kimiskidis,
709 V. K., Kugiumtzis, D., Lioumis, P., Pascual-Leone, A., Pellicciari, M. C., Rajji, T., Thut, G.,
710 Zomorodi, R., Ziemann, U., Daskalakis, Z. J. (2019). Clinical utility and prospective of
711 TMS–EEG. *Clin. Neurophysiol.*, 130(5), 802–844.
712 <https://doi.org/10.1016/j.clinph.2019.01.001>

713 Ulanov, M., Shtyrov, Y. (2022). Oscillatory beta/alpha band modulations: a potential
714 biomarker of functional language and motor recovery in chronic stroke?. *Front. Hum.*
715 *Neurosci.*, 16, 940845. <https://doi.org/10.3389/fnhum.2022.940845>

716 van Putten, M. J. (2007). The revised brain symmetry index. *Clin. Neurophysiol.*, 118(11),
717 2362-2367.

718 Westlake, K. P., Hinkley, L. B., Bucci, M., Guggisberg, A. G., Findlay, A. M., Henry, R. G.,
719 Nagarajan, S. S., Byl, N. (2012). Resting state alpha-band functional connectivity and
720 recovery after stroke. *Exp. Neurol.*, 237(1), 160–169.
721 <https://doi.org/10.1016/j.expneurol.2012.06.020>

722 Wischnewski, M., Haigh, Z. J., Shirinpour, S., Alekseichuk, I., Opitz, A. (2022). The phase
723 of sensorimotor mu and beta oscillations has the opposite effect on corticospinal excitability.
724 *Brain Stimul.*, 15(5), 1093–1100. <https://doi.org/10.1016/j.brs.2022.08.005>

725 Zhang, J. J., Fong, K. N. (2021). The modulatory effects of intermittent theta burst
726 stimulation in combination with mirror hand motor training on functional connectivity: a
727 proof-of-concept study. *Front. Neural Circuits*, 15, 548299.
728 <https://doi.org/10.3389/fncir.2021.548299>

729 Ziemann, U., Paulus, W., Nitsche, M. A., Pascual-Leone, A., Byblow, W. D., Berardelli, A.,
730 Siebner, H. R., Classen, J., Cohen, L. G., Rothwell, J. C. (2008). Consensus: motor cortex
731 plasticity protocols. *Brain Stimul.*, 1(3), 164–182. <https://doi.org/10.1016/j.brs.2008.06.006>

732 Ziemann, U., Romani, G. L., Ilmoniemi, R. J. (2019). “ConnectToBrain”: synergy project for
733 therapeutic closed-loop stimulation of brain network disorders. *Nervenarzt*, 90(8), 804–808.
734 <https://doi.org/10.1007/s00115-019-0747-x>

735 Zrenner, C., Belardinelli, P., Müller-Dahlhaus, F., Ziemann, U. (2016). Closed-loop
736 neuroscience and non-invasive brain stimulation: a tale of two loops. *Front. Cell. Neurosci.*,
737 *10*, 92. <https://doi.org/10.3389/fncel.2016.00092>

738 Zrenner, C., Desideri, D., Belardinelli, P., Ziemann, U. (2018). Real-time EEG-defined
739 excitability states determine efficacy of TMS-induced plasticity in human motor cortex.
740 *Brain Stimul.*, *11*(2), 374–389. <https://doi.org/10.1016/j.brs.2017.11.016>

741 Zrenner, C., Kozák, G., Schaworonkow, N., Metsomaa, J., Baur, D., Vetter, D., Blumberger,
742 D. M., Ziemann, U., Belardinelli, P. (2023). Corticospinal excitability is highest at the early
743 rising phase of sensorimotor μ -rhythm. *NeuroImage*, *266*, 119805.
744 <https://doi.org/10.1016/j.neuroimage.2022.119805>

745